Electronic Supplementary Information (ESI)

Differential Detection of Strong-Acids in Weak-Acids: A combination of Benzimidazole-carbazole backbone with AIE luminophores as highly sensitive and selective turn-on fluorescent probes

Pei-Chi Lin,†[a] Yu-Ting Lin,†[a] Kuan-Ting Liu,[a] Meng-Sin Chen,[a] Yong-Yun Zhang,[a] Jie-Cheng Li[b] and Man-kit Leung*[a]

[a] *Department of Chemistry and Advanced Research Center for Green Materials Science and Technology, National Taiwan University, Taipei 10617, Taiwan*
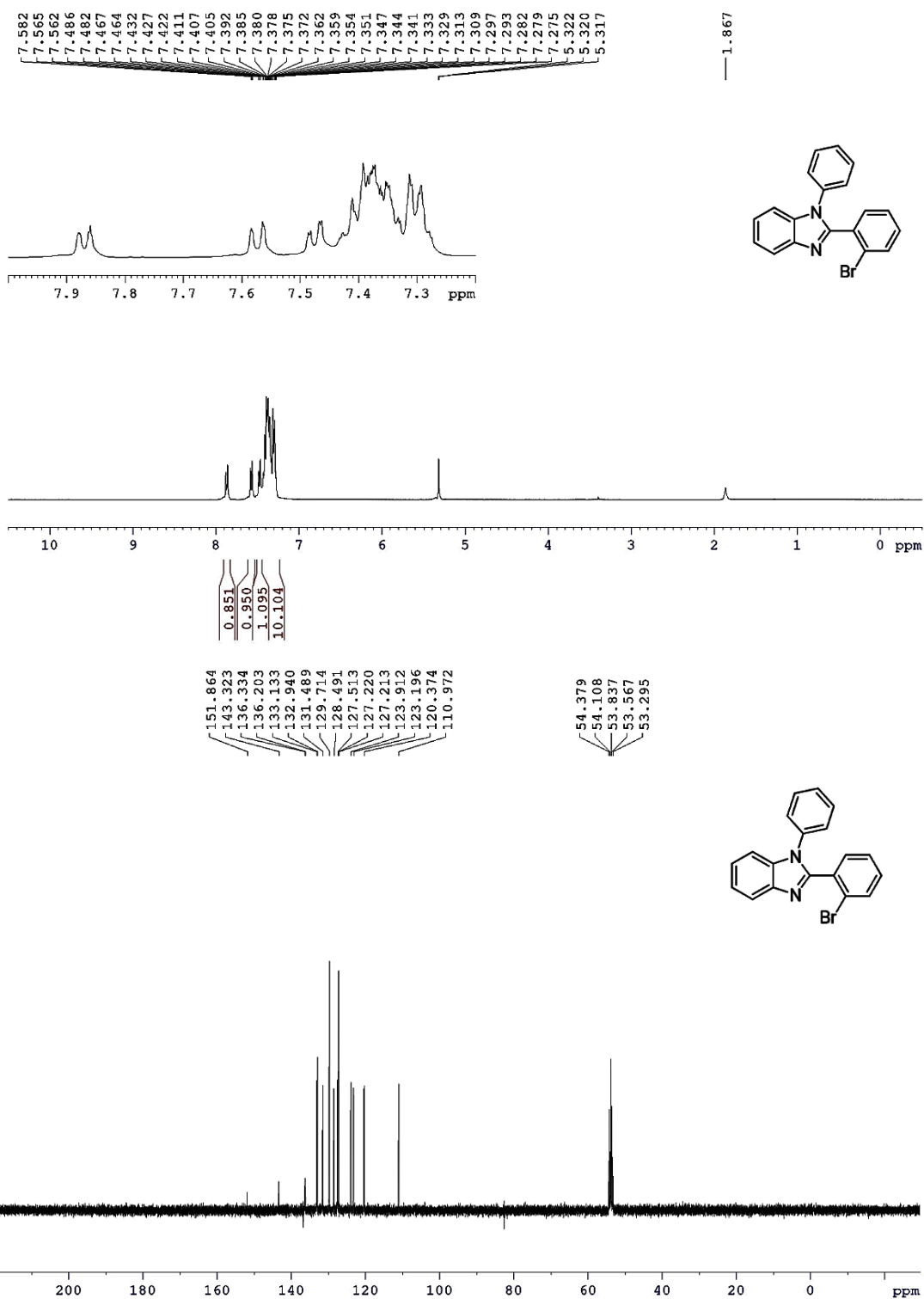
[b] *Chang Chun Plastics Co., Ltd. Kaohsiung Factory, Kaohsiung 81469, Taiwan*
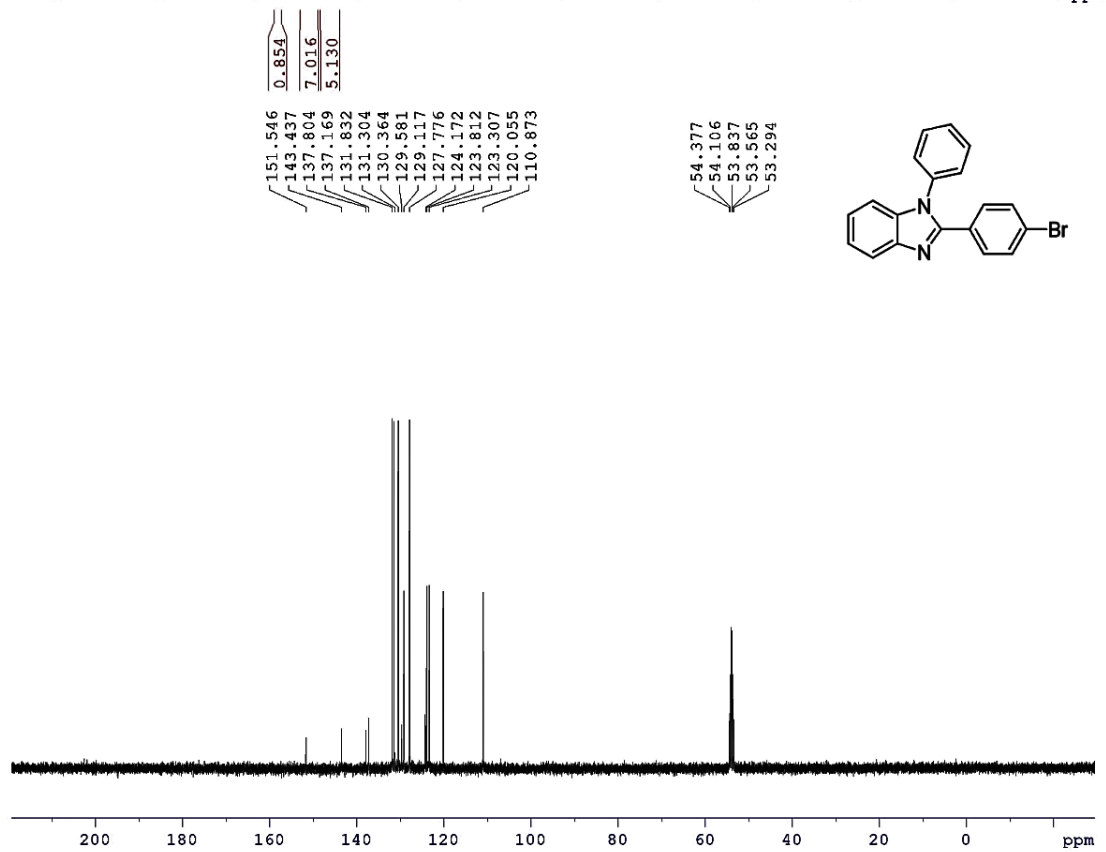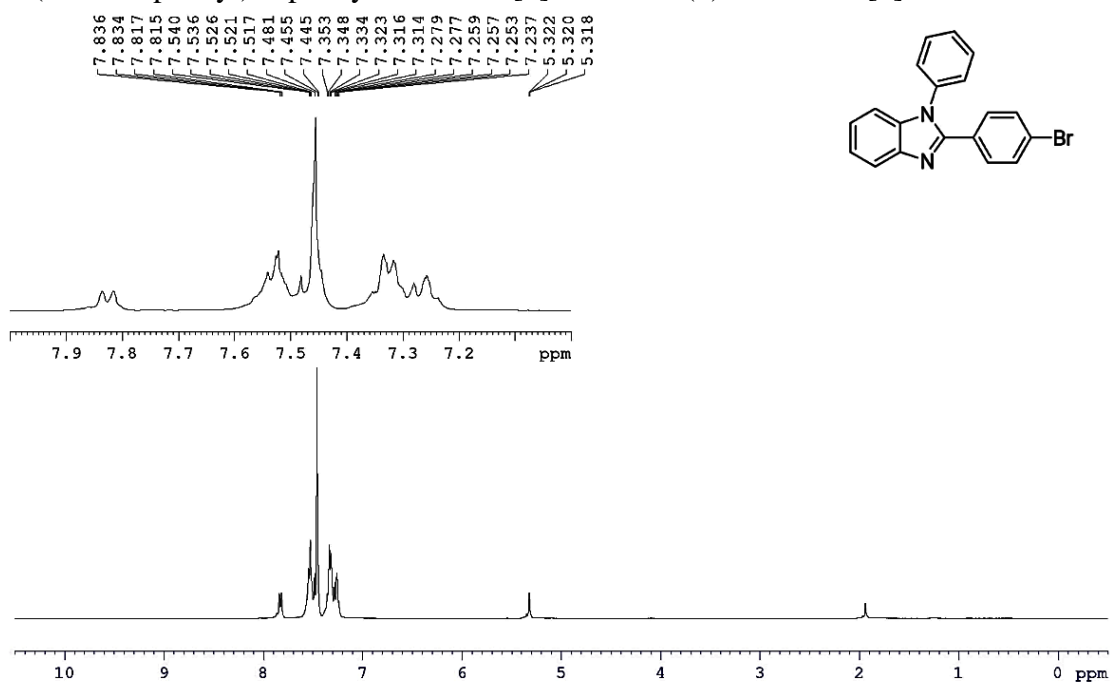
Contents

^{1}H and ^{13}C NMR spectra of each intermediate compound, *o*-BzcDPE, and *p*-BzcDPE

2-(2-bromophenyl)-1-phenyl-1H-benzo[d]imidazole (**1**) in CD$_2$Cl$_2$ [1]

2-(4-bromophenyl)-1-phenyl-1H-benzo[d]imidazole (**2**) in CD$_2$Cl$_2$ [1]

(2-bromoethene-1,1-diyl)dibenzene (**3**) in CDCl₃ [2]

9-(2,2-diphenylvinyl)-9H-carbazole **(4)** in CD$_2$Cl$_2$ [3]
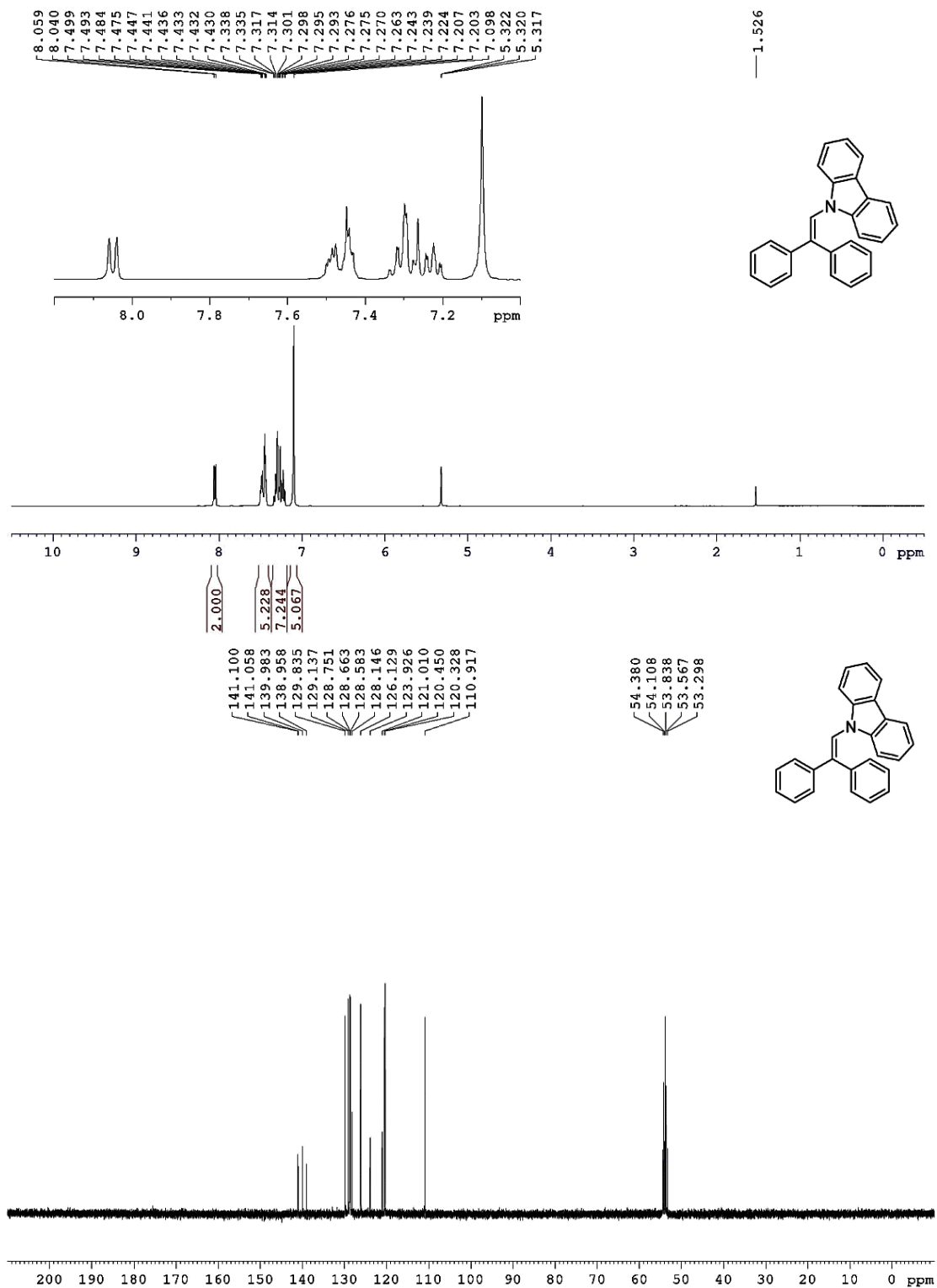
3-bromo-9-(2,2-diphenylvinyl)-9H-carbazole (**5**) in CD$_2$Cl$_2$
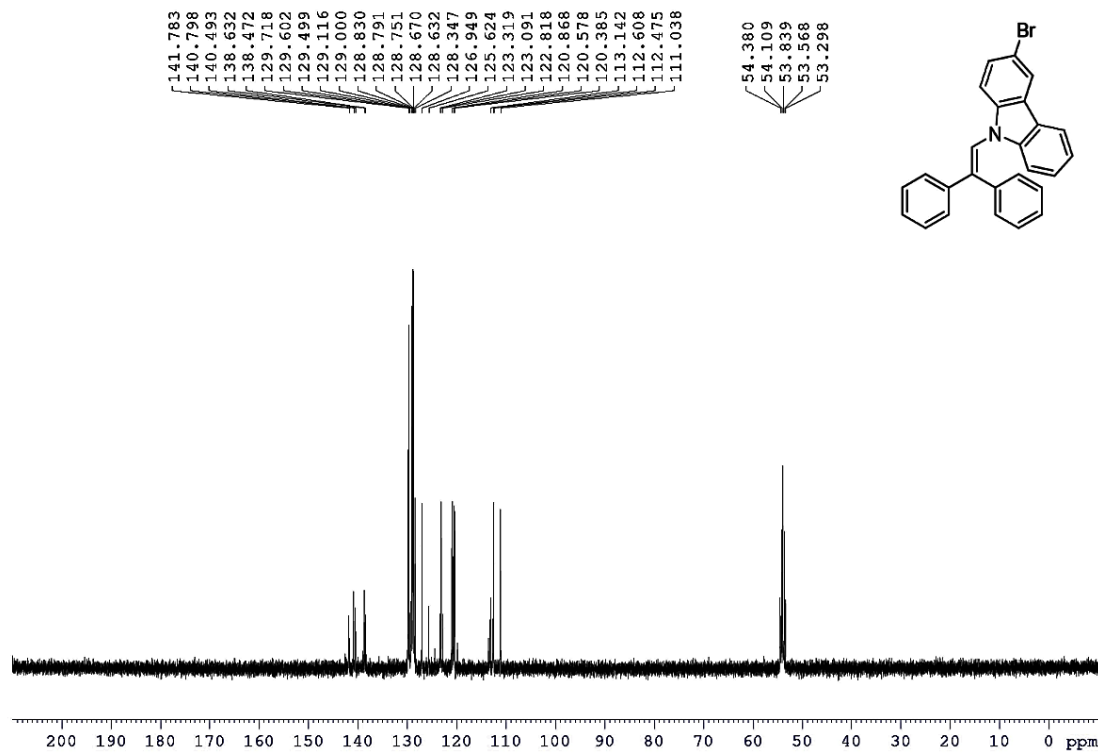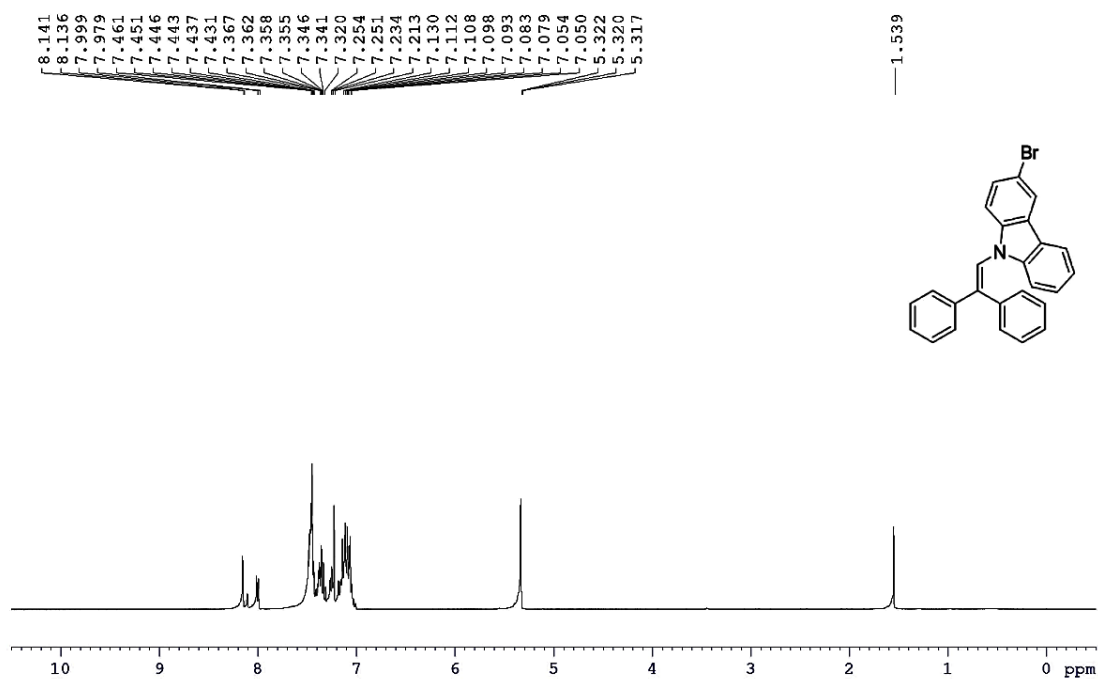
9-(2,2-diphenylvinyl)-3-(4,4,5,5-tetramethyl-1,3,2-dioxaborolan-2-yl)-9H-carbazole
(6) in (CD$_3$)$_2$CO
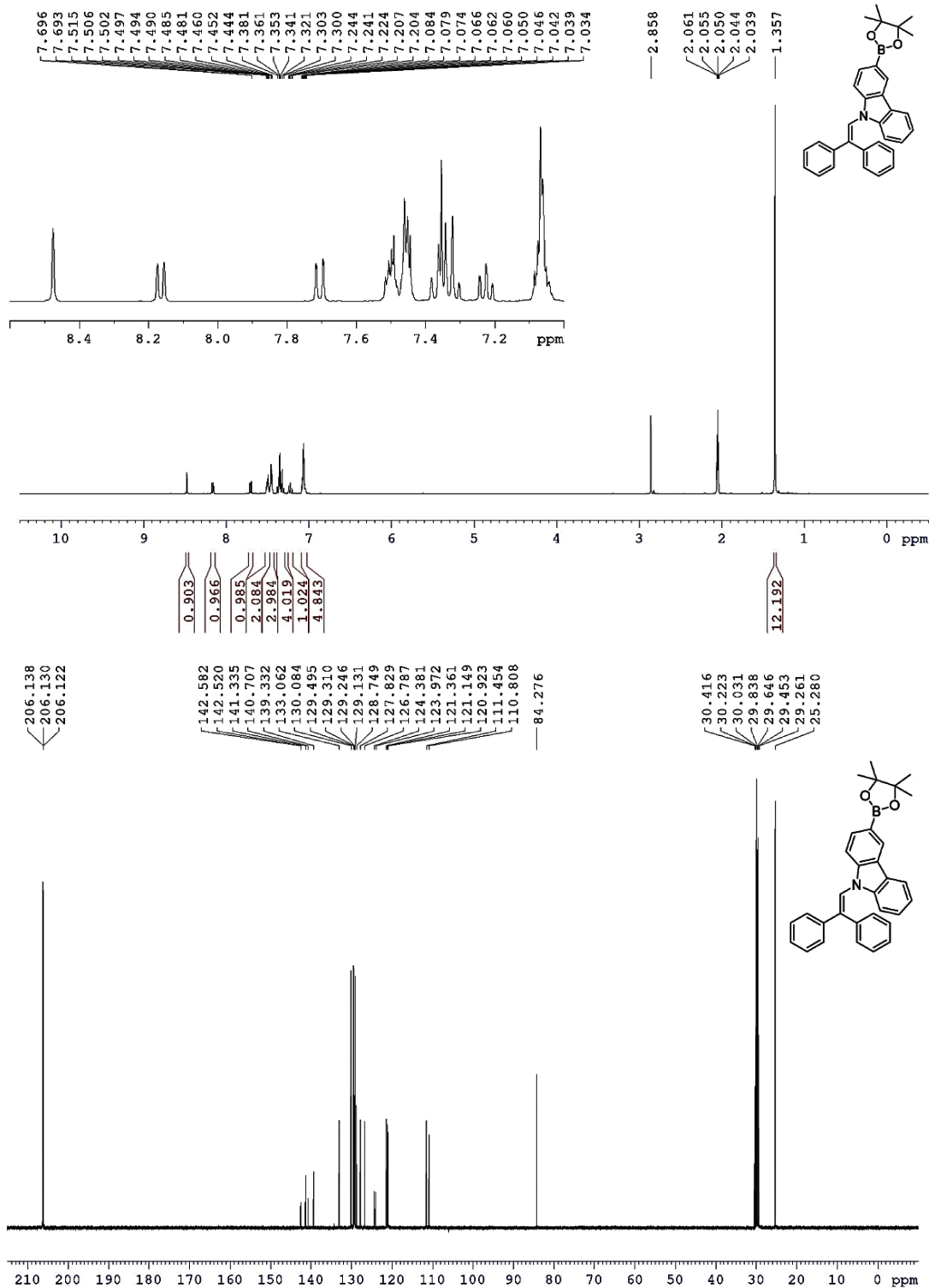
9-(2,2-diphenylvinyl)-3-(2-(1-phenyl-1H-benzo[d]imidazol-2-yl)phenyl)-9H-carbazole (**o-BzcDPE**) in CD_2Cl_2
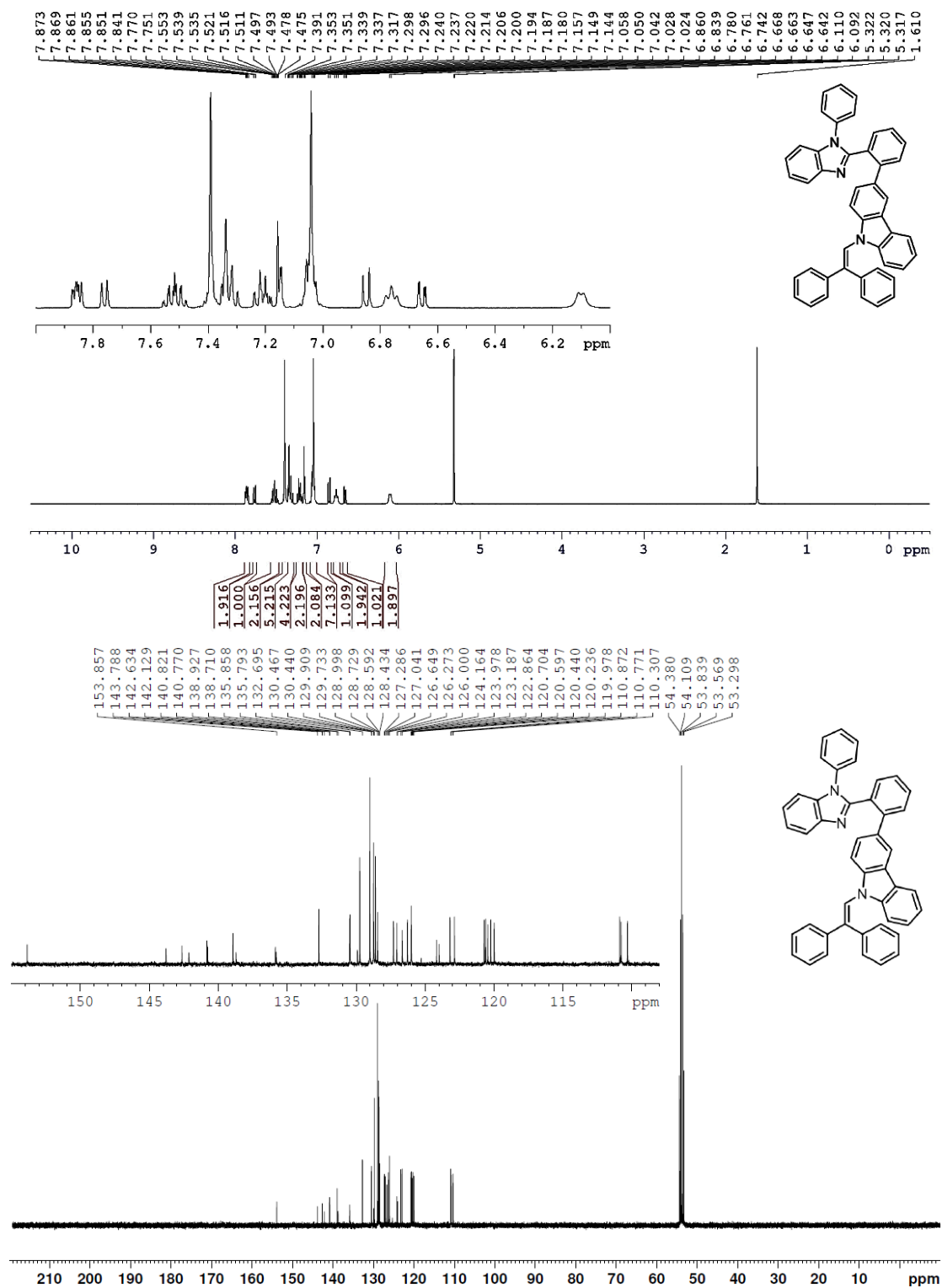
9-(2,2-diphenylvinyl)-3-(4-(1-phenyl-1H-benzo[d]imidazol-2-yl)phenyl)-9H-carbazole (**p-BzcDPE**) in CDCl₃
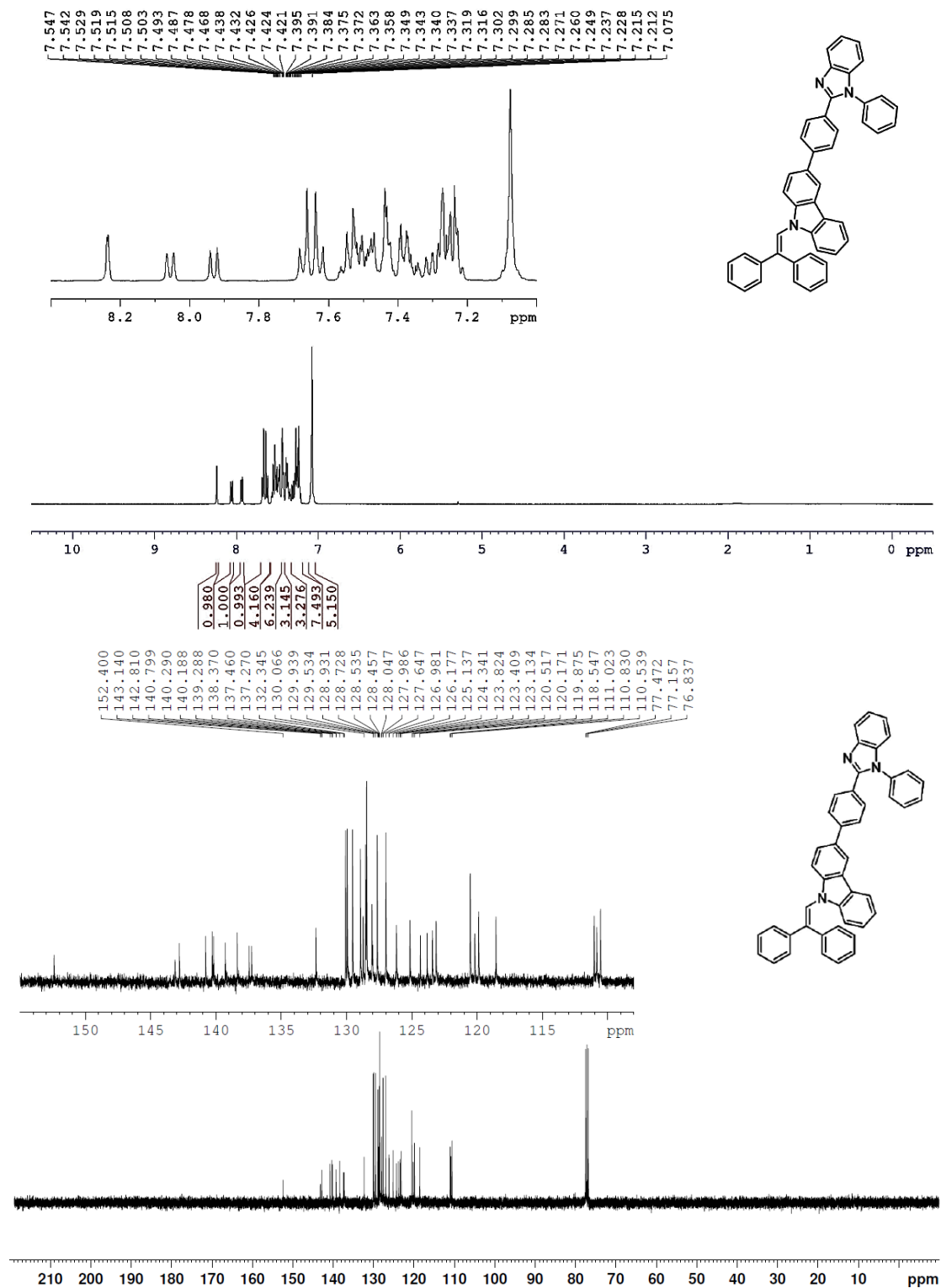
HRMS of each intermediate compound, *o*-BzcDPE, and *p*-BzcDPE
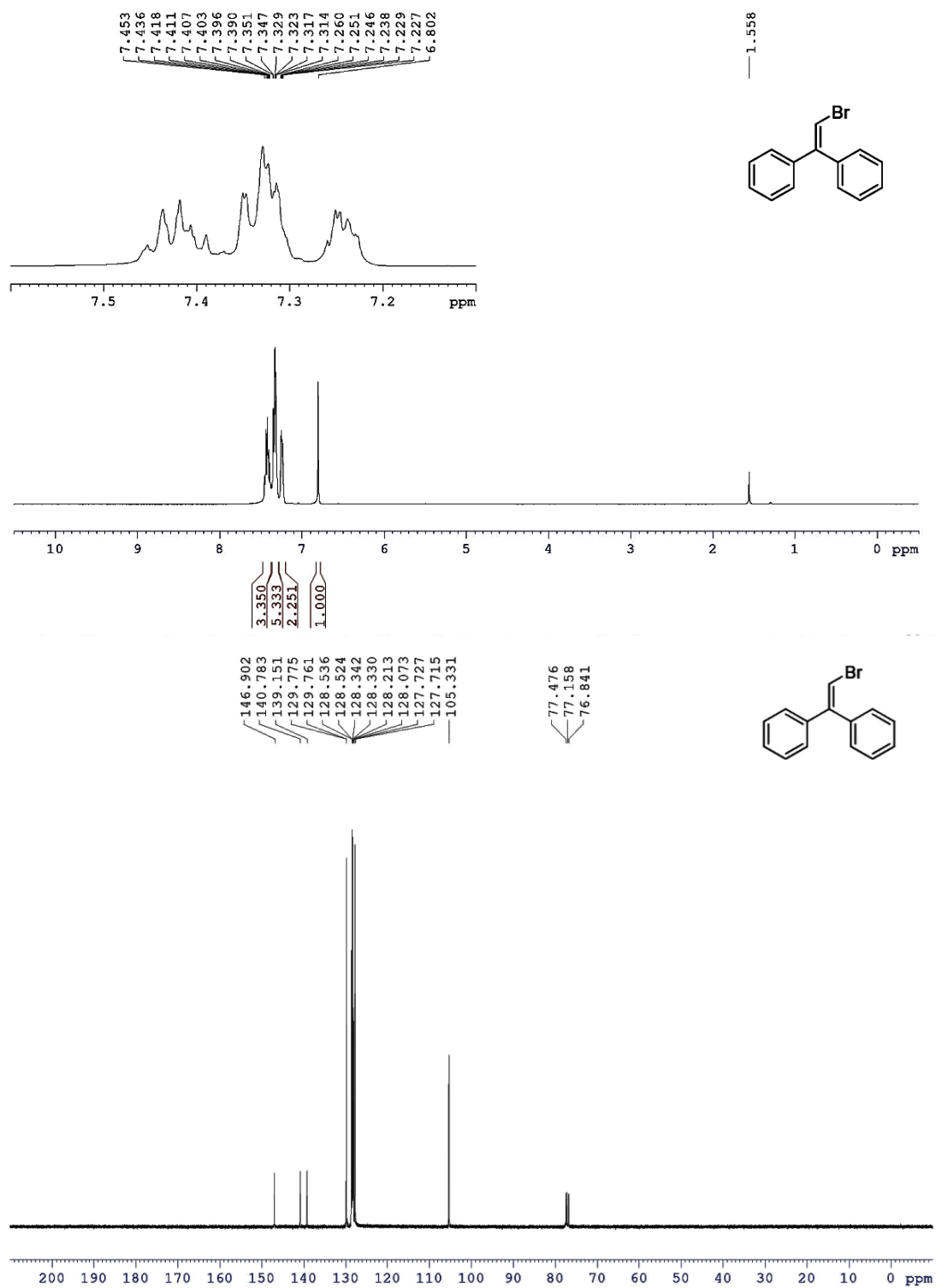
2-(2-bromophenyl)-1-phenyl-1H-benzo[d]imidazole **(1)**
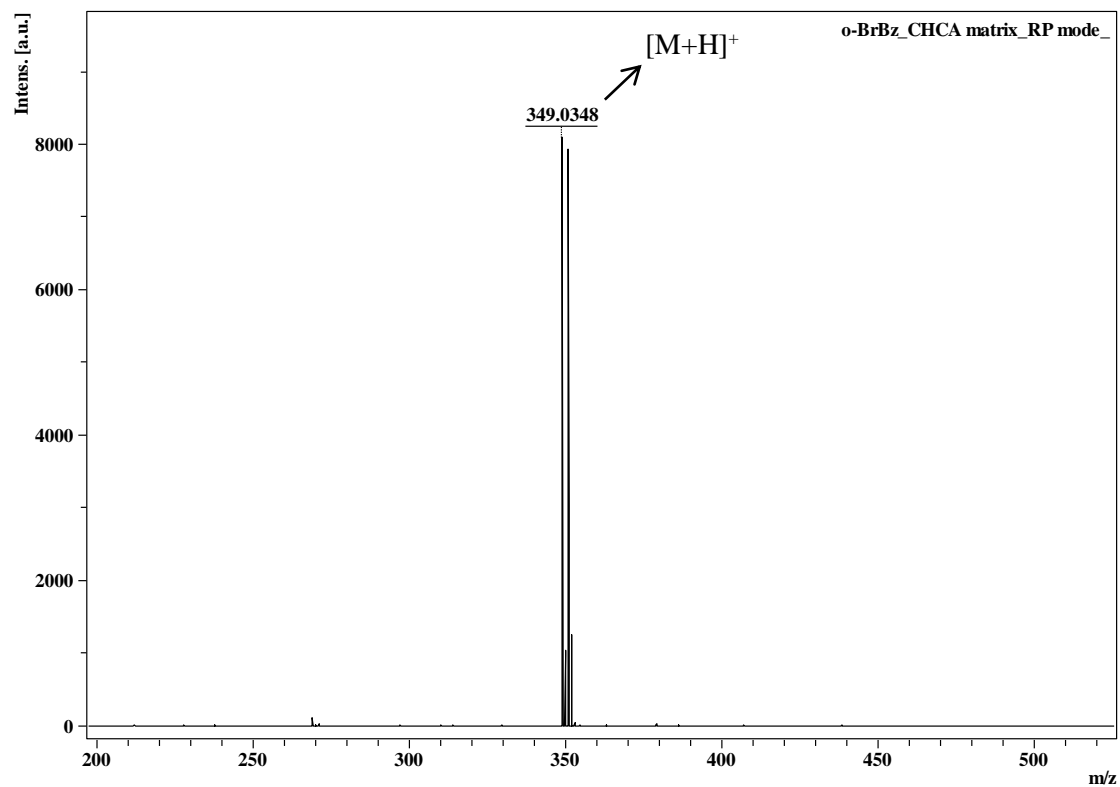
2-(4-bromophenyl)-1-phenyl-1H-benzo[d]imidazole (**2**)
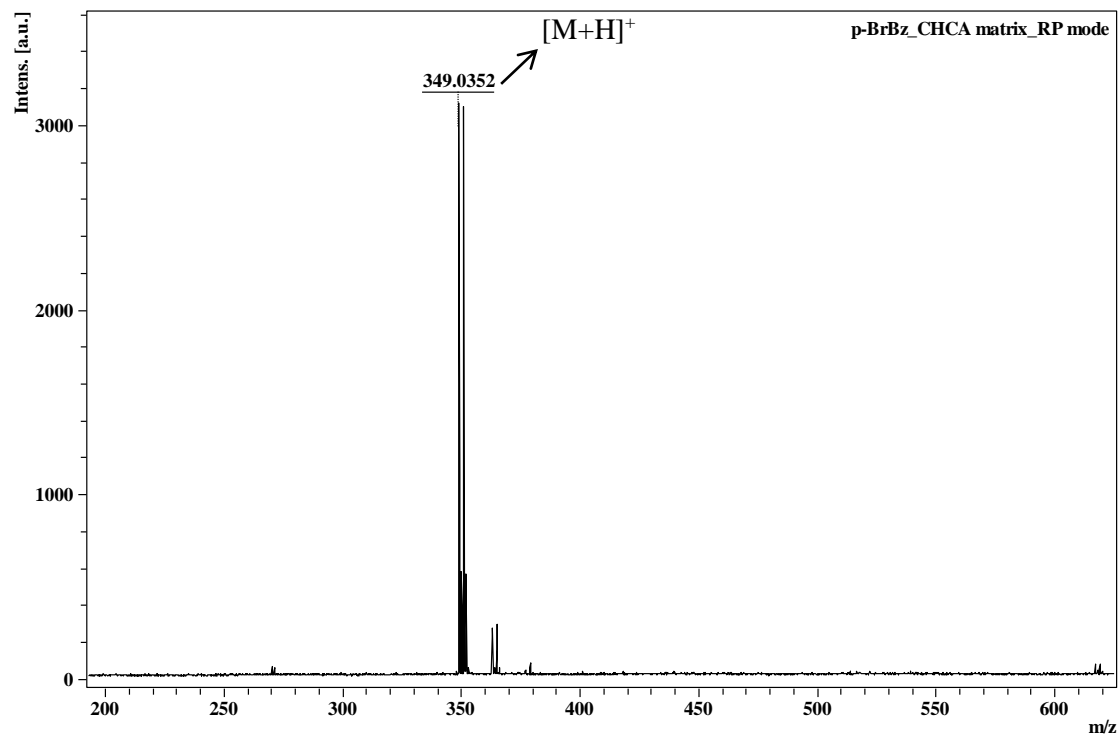
9-(2,2-diphenylvinyl)-9H-carbazole (**4**)
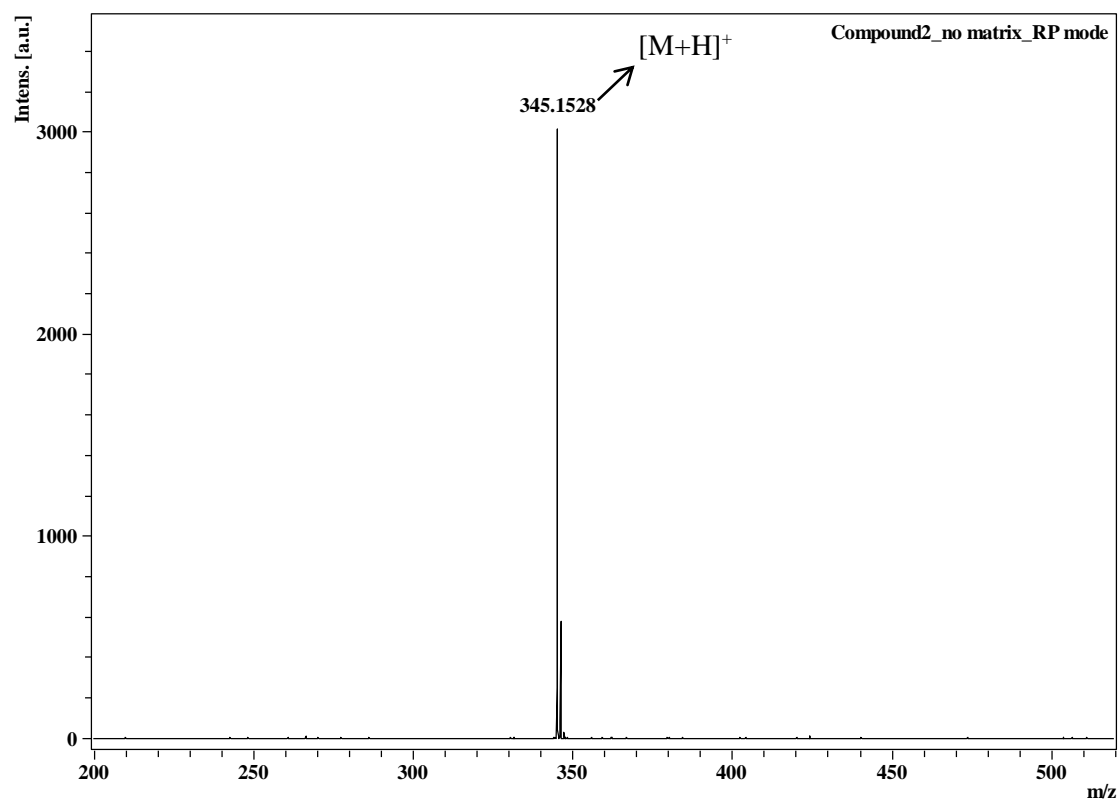
3-bromo-9-(2,2-diphenylvinyl)-9H-carbazole (**5**)
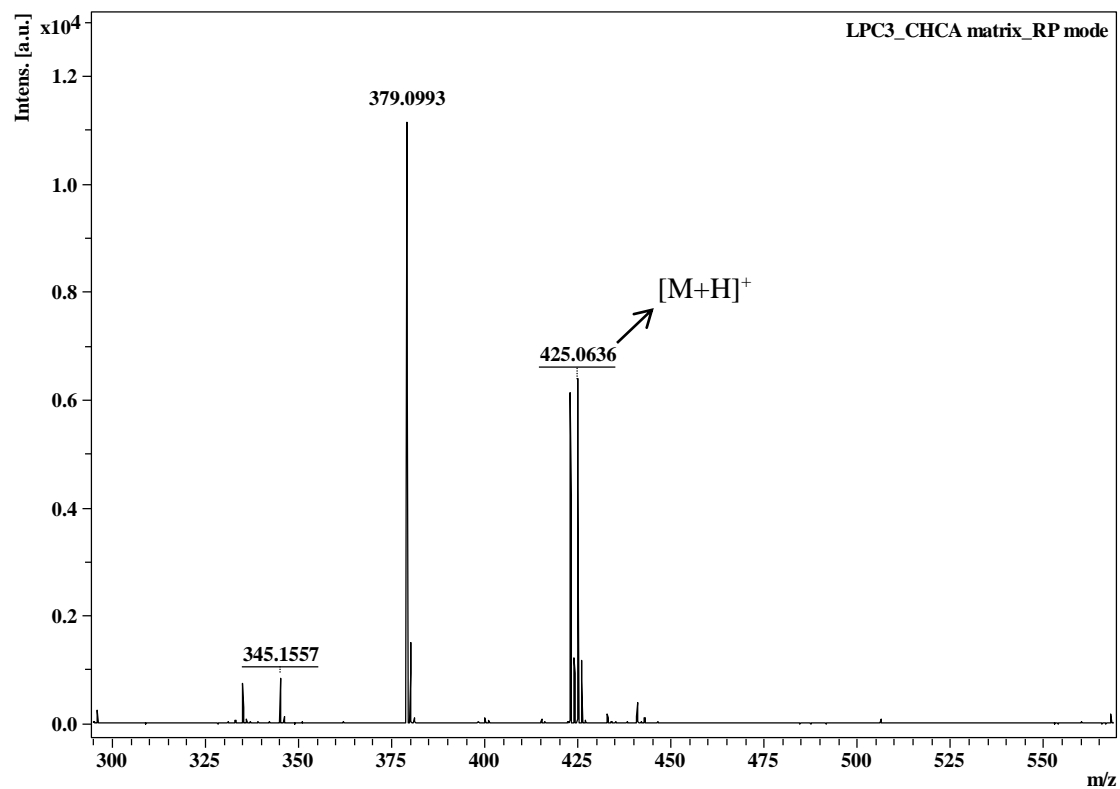
9-(2,2-diphenylvinyl)-3-(4,4,5,5-tetramethyl-1,3,2-dioxaborolan-2-yl)-9H-carbazole **(6)**
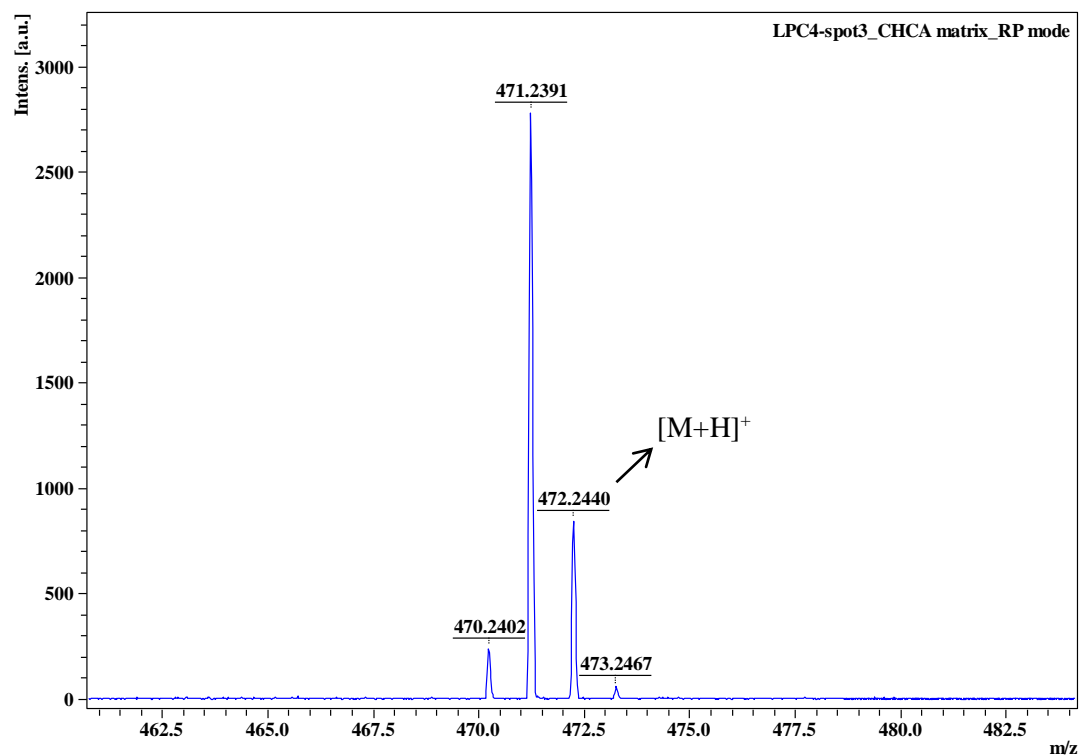
9-(2,2-diphenylvinyl)-3-(2-(1-phenyl-1H-benzo[d]imidazol-2-yl)phenyl)-9H-carbazole (*o*-**BzcDPE**)
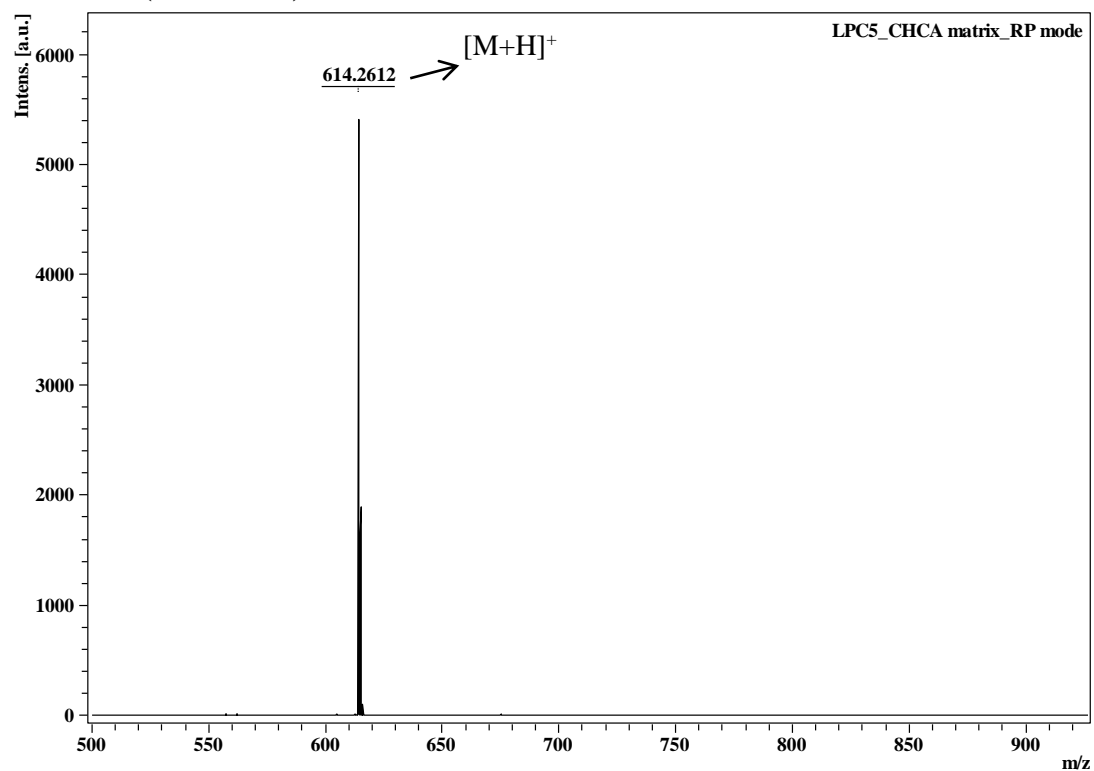
9-(2,2-diphenylvinyl)-3-(4-(1-phenyl-1H-benzo[d]imidazol-2-yl)phenyl)-9H-carbazole (*p*-BzcDPE)
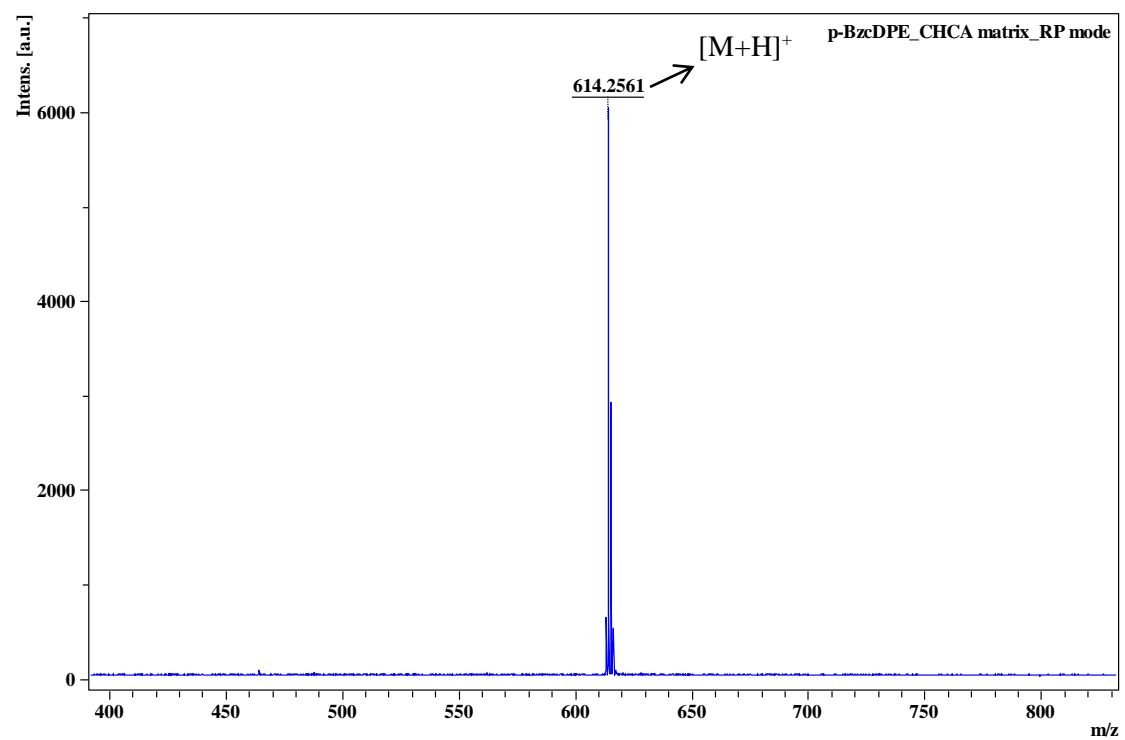
Crystal data of *o*-BzcDPE, *p*-BzcDPE, and *p*-BzcDPE+HCl
Table S1

Crystal data and structure refinement for *p*-BzcDPE.

|	
Empirical formula	$C_{45}H_{31}N_3$
Formula weight	613.73
Crystal system	Triclinic
Space group	P-1
Unit cell dimensions	a = 8.9933(13) Å α= 82.180(12)°.
	b = 9.9705(15) Å β= 81.467(12)°.
	c = 19.962(3) Å γ= 63.224(14)°.
Volume	1575.5(4) Å^3
Z	2
F(000)	644
Density (calculated)	1.294 Mg/m^3
Wavelength	0.71073 Å
Cell parameters reflections used	2837
Theta range for Cell parameters	3.7430 to 29.3880°.
Absorption coefficient	0.076 mm^{-1}
Temperature	200(2) K
Crystal size	0.25 x 0.20 x 0.15 mm^3
	Data collection
Diffractometer	Xcalibur, Atlas, Gemini
Absorption correction	Semi-empirical from equivalents
Max. and min. transmission	1.00000 and 0.82855
No. of measured reflections	10313
No. of independent reflections	10313 [R(int) = 0.1505]
No. of observed [I>2_igma(I)]	6857
Completeness to theta = 25.242°	99.8 %
Theta range for data collection	2.844 to 27.498°.
	Refinement
Final R indices [I>2sigma(I)]	R1 = 0.0741, wR2 = 0.1969
R indices (all data)	R1 = 0.1110, wR2 = 0.2208
Goodness-of-fit on F^2	1.356
No. of reflections	10313
No. of parameters	434
No. of restraints	0
Largest diff. peak and hole	0.304 and -0.352 e.Å^{-3}

Table S2

Crystal data and structure refinement for ***p*-BzcDPE+HCl** (The solvent disorder was squeezed by the program. PLATON.)

Empirical formula	$C_{45}H_{32}ClN_3$	
Formula weight	650.18	
Crystal system	Triclinic	
Space group	P-1	
Unit cell dimensions	a = 9.1375(11) Å	α= 77.293(8)°.
	b = 11.3158(13) Å	β= 86.737(8)°.
	c = 18.3796(13) Å	γ=81.617(10)°.
Volume	1833.5(3) Å^3	
Z	2	
F(000)	680	
Density (calculated)	1.178 Mg/m^3	
Wavelength	0.71073 Å	
Cell parameters reflections used	5155	
Theta range for Cell parameters	3.3080 to 31.8950°.	
Absorption coefficient	0.139 mm^{-1}	
Temperature	100(2) K	
Crystal size	0.20 x 0.20 x 0.15 mm^3	
	Data collection	
Diffractometer	Xcalibur, Atlas, Gemini	
Absorption correction	Semi-empirical from equivalents	
Max. and min. transmission	1.00000 and 0.40975	
No. of measured reflections	18358	
No. of independent reflections	8411 [R(int) = 0.0751]	
No. of observed [I>2_igma(I)]	5417	
Completeness to theta = 25.242°	99.8 %	
Theta range for data collection	3.120 to 27.499°.	
	Refinement	
Final R indices [I>2sigma(I)]	R1 = 0.0685, wR2 = 0.1694	
R indices (all data)	R1 = 0.1042, wR2 = 0.2063	
Goodness-of-fit on F^2	1.024	
No. of reflections	8411	
No. of parameters	473	
No. of restraints	372	
Largest diff. peak and hole	0.608 and -0.830 e.Å^{-3}	

Table S3

Crystal data and structure refinement for *o*-**BzcDPE**.

Empirical formula	$C_{45}H_{31}N_3$
Formula weight	613.73
Crystal system	Triclinic
Space group	P-1
Unit cell dimensions	a = 9.7546(3) Å α= 97.964(2)°.
	b = 10.8555(3) Å β= 92.592(2)°.
	c = 17.1955(5) Å γ= 115.717(3)°.
Volume	1613.31(9) Å^3
Z	2
F(000)	644
Density (calculated)	1.263 Mg/m^3
Wavelength	0.71073 Å
Cell parameters reflections used	3529
Theta range for Cell parameters	3.4370 to 27.3820°.
Absorption coefficient	0.074 mm^{-1}
Temperature	100(2) K
Crystal size	0.20 x 0.15 x 0.10 mm^3
	Data collection
Diffractometer	Xcalibur, Atlas, Gemini
Absorption correction	Semi-empirical from equivalents
Max. and min. transmission	1.00000 and 0.94534
No. of measured reflections	13449
No. of independent reflections	7149 [R(int) = 0.0430]
No. of observed [I>2_igma(I)]	4255
Completeness to theta = 25.242°	99.8 %
Theta range for data collection	2.913 to 27.499°.
	Refinement
Final R indices [I>2sigma(I)]	R1 = 0.0603, wR2 = 0.1235
R indices (all data)	R1 = 0.1208, wR2 = 0.1658
Goodness-of-fit on F^2	0.924
No. of reflections	7149
No. of parameters	433
No. of restraints	0
Largest diff. peak and hole	0.275 and -0.244 e.Å^{-3}

NMR spectra assignments of *o*-BzcDPE
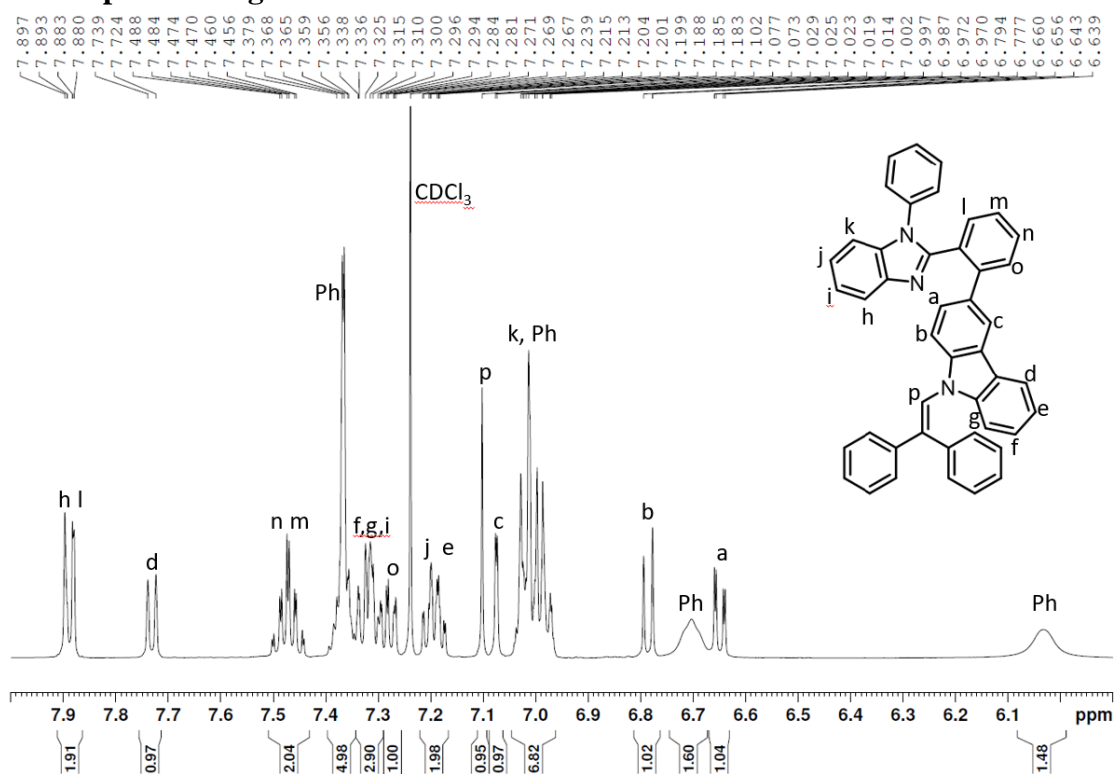
Fig. S1. ^{1}H NMR spectra assignments of *o*-**BzcDPE**
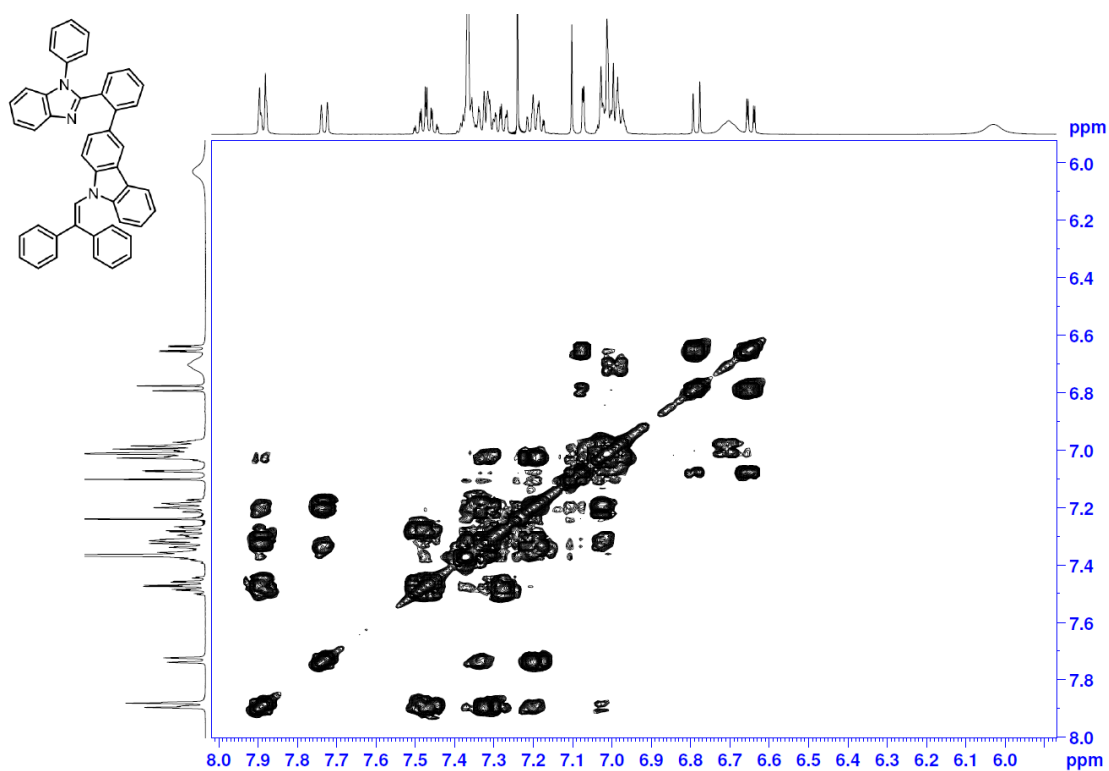

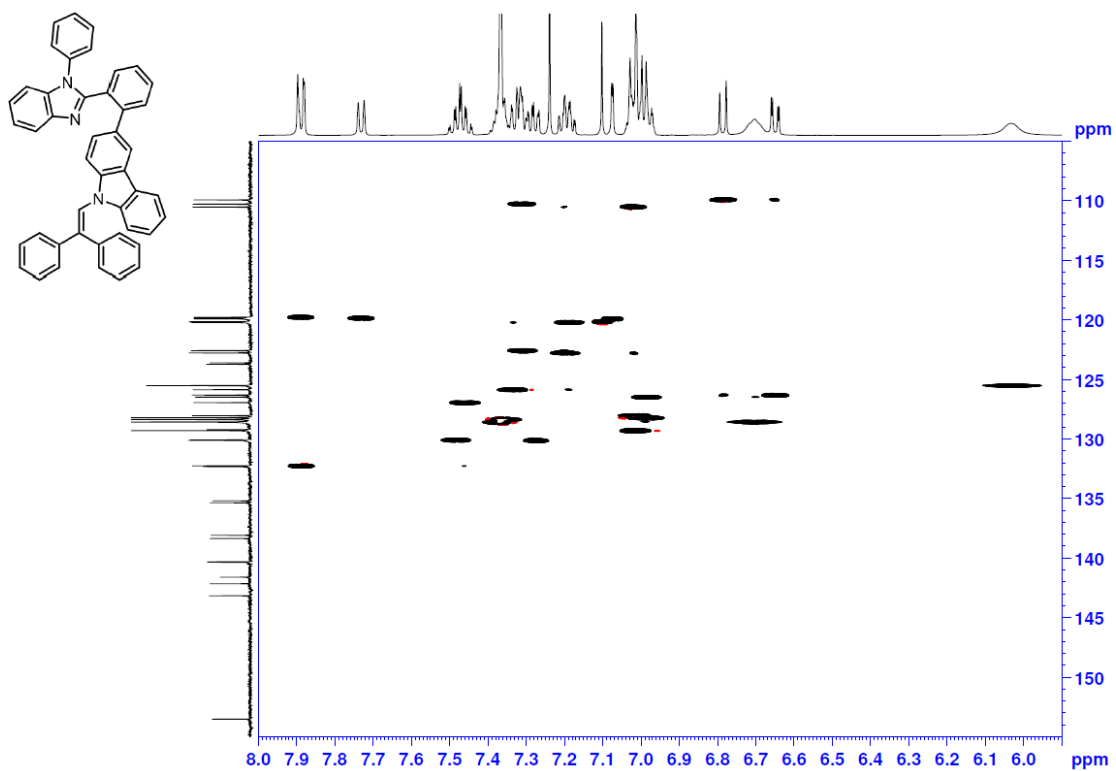**Fig. S2.** ^{1}H-^{1}H COSY NMR spectra of *o*-**BzcDPE**
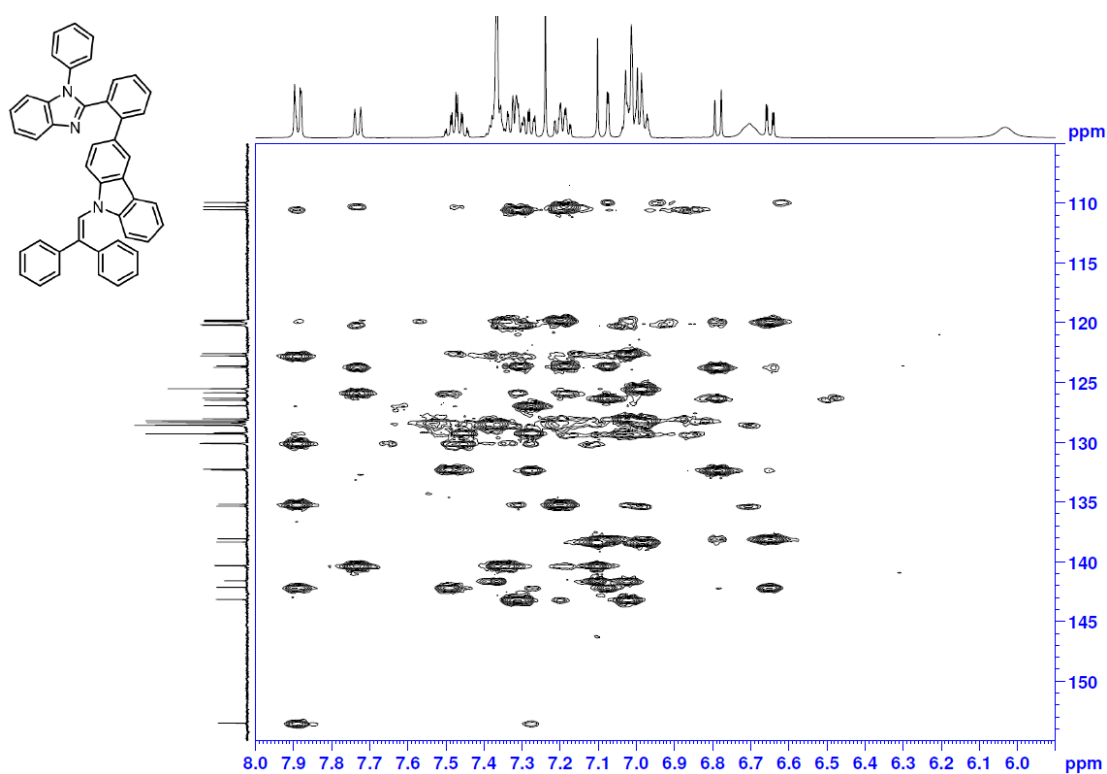
Fig. S3. HSQC NMR spectra of *o*-BzcDPE

Fig. S4. HMBC NMR spectra of *o*-BzcDPE

Oscillator strength data for DFT studies

All calculations were performed using the parameters in toluene. The structures of *o*-**BzcDPE**, *p*-**BzcDPE** and *o*-**BzcDPE**+**H**$^+$ **Cl**$^-$ were optimized using the described DFT routines. The calculated spectral transitions of *p*-**BzcDPE**+**H**$^+$ **Cl**$^-$ are based on the crystallographic structure provided in this paper. All the first major electronic transitions with reasonable oscillator strength (*f*) arise from the HOMO to LUMO transitions.

Table S4

	Electronic transition	λ_{abs} (nm)	E_{ex} (eV)	Oscillator strength, f	Major contributions[a]
o-**BzcDPE**[b]	$S_0 \rightarrow S_1$	360.68	3.4376	0.5125	H $\rightarrow$ L (70%)
	$S_0 \rightarrow S_2$	331.78	3.7369	0.0522	H $\rightarrow$ L+1 (69%)
	$S_0 \rightarrow S_3$	324.24	3.8238	0.0098	H $\rightarrow$ L+2 (68%)
p-**BzcDPE**[b]	$S_0 \rightarrow S_1$	367.79	3.3711	0.9031	H $\rightarrow$ L (67%), H $\rightarrow$ L+1 ($-$20%)
	$S_0 \rightarrow S_2$	341.37	3.6320	0.4355	H $\rightarrow$ L (20%), H $\rightarrow$ L+1 (66%)
	$S_0 \rightarrow S_3$	327.03	3.7913	0.0262	H $\rightarrow$ L+2 (65%)
o-**BzcDPE**+**H**$^{+c}$	$S_0 \rightarrow S_1$	381.67	3.2485	0.1747	H $\rightarrow$ L (69%)
	$S_0 \rightarrow S_2$	357.15	3.4715	0.2955	H $\rightarrow$ L+1 (69%)
	$S_0 \rightarrow S_3$	346.80	3.5751	0.0021	H$-$2 $\rightarrow$ L (34%), H$-$1 $\rightarrow$ L (62%)
p-**BzcDPE**+**H**$^{+c}$	$S_0 \rightarrow S_1$	454.59	2.7274	0.0465	H$-$2 $\rightarrow$ L (21%), H$-$1 $\rightarrow$ L (65%) , H $\rightarrow$ L (19%)
	$S_0 \rightarrow S_2$	451.93	2.7435	0.0104	H$-$2 $\rightarrow$ L (67%), H$-$1 $\rightarrow$ L ($-$20%)
	$S_0 \rightarrow S_3$	445.74	2.7816	0.6438	H$-$1 $\rightarrow$ L ($-$20%), H $\rightarrow$ L (67%)

[a] H = HOMO; L = LUMO; only contributions above 15% are included.

[b] Calculated by TD-DFT//B3LYP/6-31G (d)

[c] Calculated by TD-DFT//B3LYP/6-31+G (d)

UV-Vis absorption of *o*-BzcDPE, *p*-BzcDPE, *o*-BzcDPE+H$^+$, and *p*-BzcDPE+H$^+$ in different solvents.
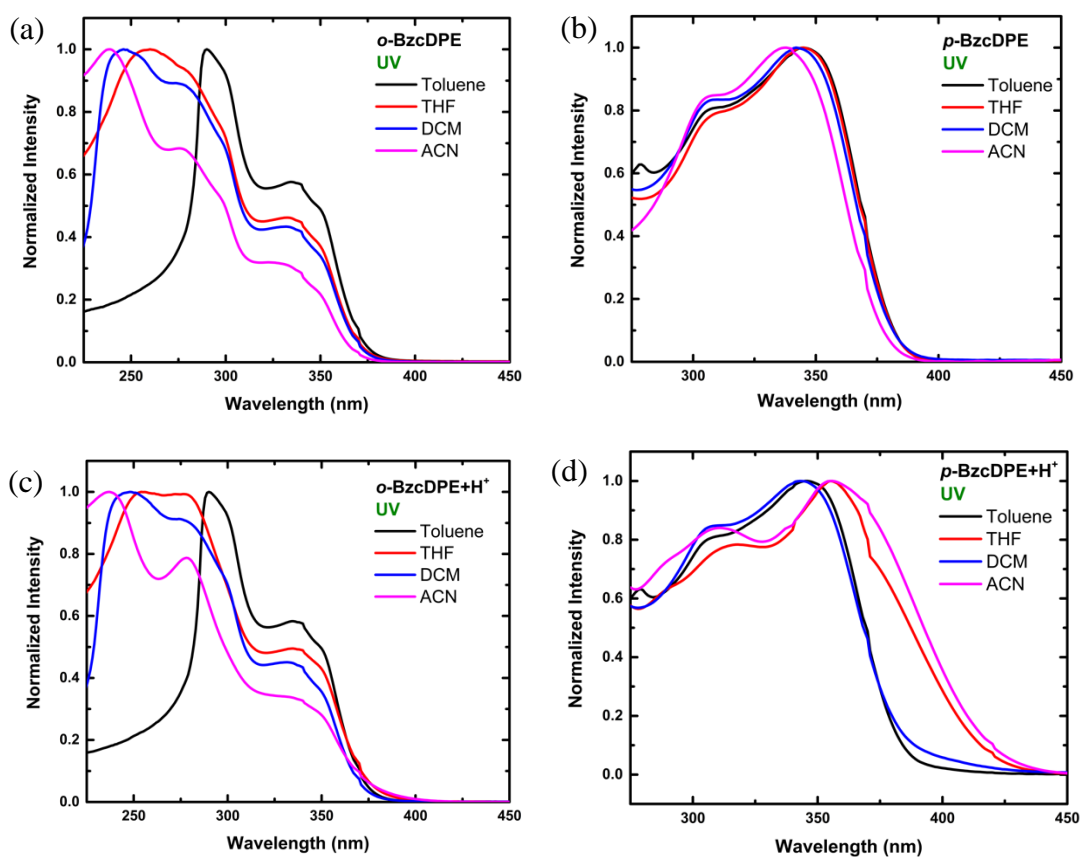
Fig. S5. UV-Vis absorption of (a) *o*-BzcDPE, (b) *p*-BzcDPE, (c) *o*-BzcDPE+H$^+$, and (d) *p*-BzcDPE+H$^+$ in toluene, THF, DCM, and ACN (1 mM), respectively.

Solvato-fluorochromism of *o*-BzcDPE, *p*-BzcDPE, *o*-BzcDPE+H$^+$, and *p*-BzcDPE+H$^+$ in different solvents.
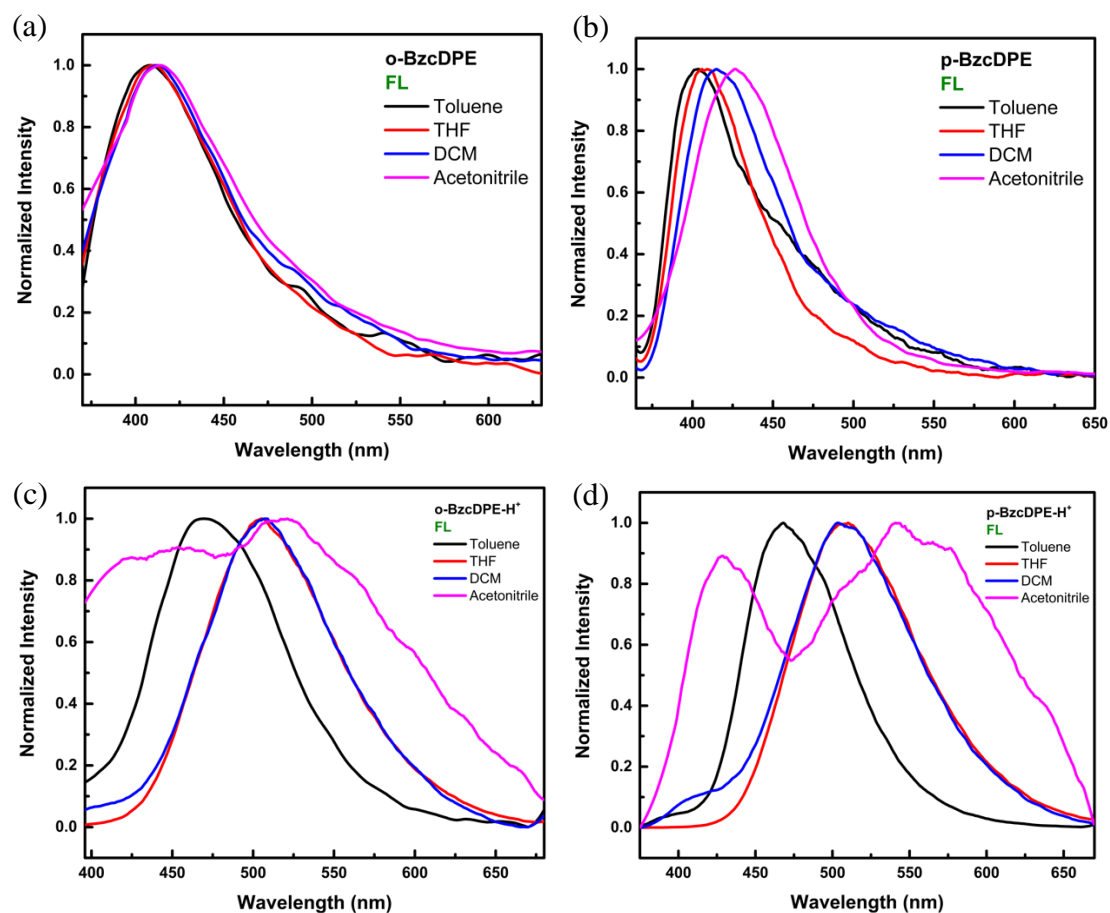
Fig. S6. Solvato-fluorochromism of (a) *o*-**BzcDPE**, (b) *p*-**BzcDPE**, (c) *o*-**BzcDPE**+H$^+$, and (d) *p*-**BzcDPE**+H$^+$ in toluene, DCM, THF, and ACN (1 mM), respectively. The data are smoothed for better identification.
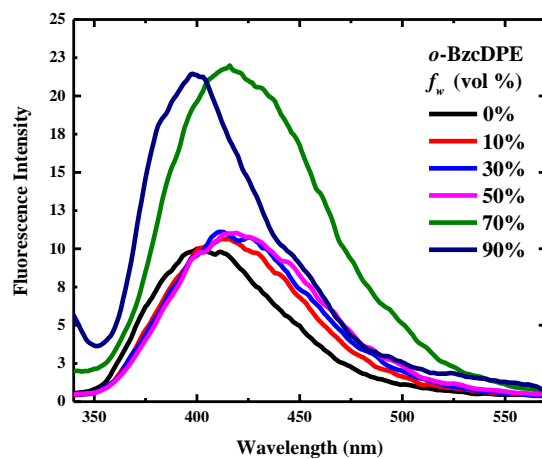
Study of AIE phenomenon of *o*-BzcDPE

Fig. S7. Fluorescence spectra of ***o*-BzcDPE** (λ_{ex} = 320 nm) at 1.0×10^{-4} M in THF-H$_2$O mixture with f_w (vol%) : 0, 10, 30, 50, 70 and 90, respectively.

Optical titration of sulfuric acid

Table S5

The preparation of solution for the spectrophotometric titration of sulfuric acid.

The amount of sulfuric acid (ppm)	3.0 mM of indicator (mL)	3.0 mM of sulfuric solution (mL)	Toluene (mL)	Total volume (mL)
0	1.00	0	2.00	
15	1.00	0.15	1.85	
29	1.00	0.30	1.70	
44	1.00	0.45	1.55	
59	1.00	0.60	1.40	
74	1.00	0.75	1.25	
88	1.00	0.90	1.10	3.00
104	1.00	1.05	0.95	
118	1.00	1.20	0.80	
132	1.00	1.35	0.65	
147	1.00	1.50	0.50	
162	1.00	1.65	0.35	
177	1.00	1.80	0.20	
191	1.00	1.95	0.05	

The calculation of the amount of sulfuric acid

In order to express the amount of sulfuric acid as parts per million (ppm), we assumed that the density of the mixed solution was 1.0 g/mL. Herein, we took 15 ppm for example, and the calculation method was shown below.

$$\frac{3 \text{ (mM) } H_2SO_4 \text{ toluene solution} \times 0.15 \text{ (mL)}}{3 \text{ (mL)}} = 0.15 \text{ (mM)} = 1.5 \times 10^{-4} \left(\frac{mole}{L}\right)$$

$$= 1.5 \times 10^{-4} \left(\frac{mole}{kg}\right) = 1.5 \times 10^{-4} \left(\frac{mole}{kg}\right) \times 98.08 \left(\frac{g}{mole}\right) = 14.712 \left(\frac{mg}{kg}\right) \approx 15 \text{ ppm}$$
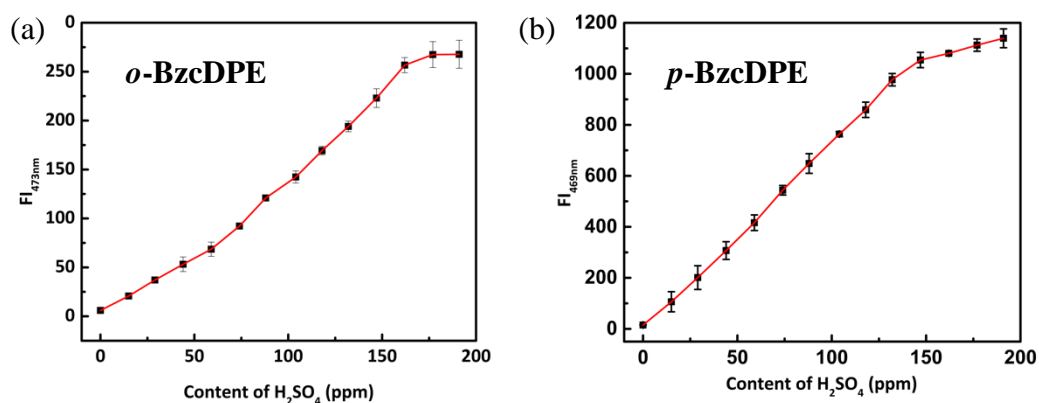
Fig. S8. Plots of the mean and standard deviation of (a)*o*-BzcDPE and (b)*p*-BzcDPE between fluorescence intensity and content of H_2SO_4 after repeating the titration experiment three times.

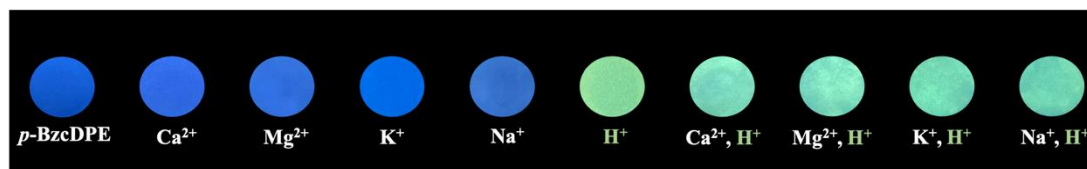**Fig. S9.** The photograph of *p*-BzcDPE pre-stained filter paper in the presence of different cations solution (1 mM) only and coexisting with H^+ (1 mM) under UV light (365 nm).
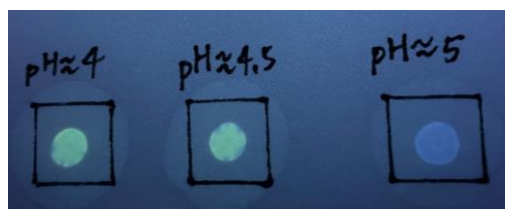

Fig. S10. The sensing performance of *p*-BzcDPE pre-stained filter paper with pH values ranging from 4 to 5 under UV light (365 nm).

Fig. S11. Regeneration of *p*-BzcDPE pre-stained filter paper under UV light (365 nm).

Optical titration of PFOA

Table S6

The preparation of solution for the spectrophotometric titration of PFOA.

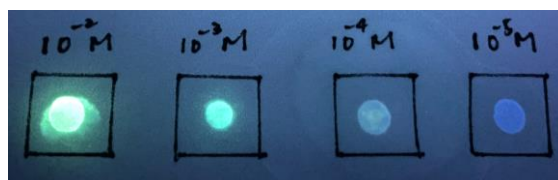| The concentration of PFOA(mM)	15 mM of octanoic acid solution (mL)	1.0 mM of PFOA solution (mL)	1.0 mM of indicator (mL)	Toluene (mL)	Total volume (mL)
0	1.33	0	0.10	0.57	
0.01	1.33	0.02	0.10	0.55	
0.02	1.33	0.04	0.10	0.53	
0.03	1.33	0.06	0.10	0.51	
0.04	1.33	0.08	0.10	0.49	
0.05	1.33	0.10	0.10	0.47	2.00
0.06	1.33	0.12	0.10	0.45	
0.07	1.33	0.14	0.10	0.43	
0.08	1.33	0.16	0.10	0.41	
0.09	1.33	0.18	0.10	0.39	
0.10	1.33	0.20	0.10	0.37	

Fig. S12. Sensing performance of *p*-BzcDPE pre-stained filter paper in the presence of aqueous PFOA solutions with different concentration under UV light (365 nm).

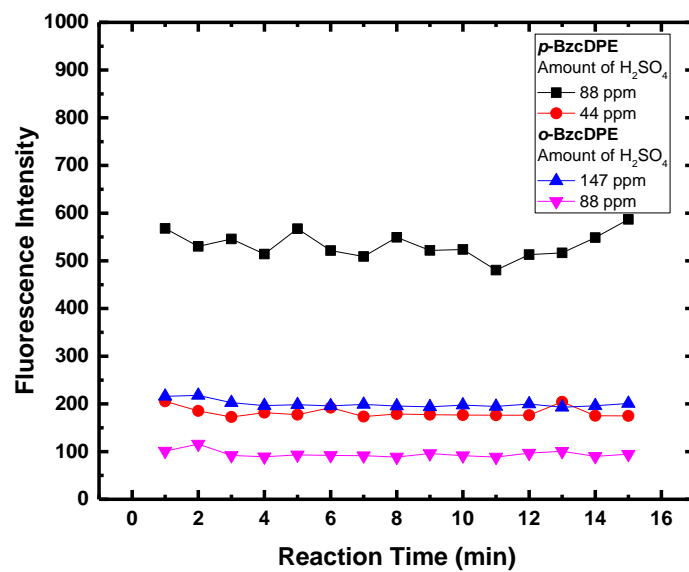**Time response and stability tests of *o*-BzcDPE and *p*-BzcDPE under different acid conditions.**

Fig. S13. The fluorescence intensity versus reaction time of ***o*-BzcDPE** (1 mM) and ***p*-BzcDPE** (1 mM) under different amounts of H_2SO_4.

Quantum yield calculation and data of *o*-BzcDPE+H$^+$ and *p*-BzcDPE+H$^+$ in different solvent.

Herein, we took coumarin 6 as the reference compound for our quantum yield measurement. According to related literature, the calculation method we used was shown below [4].

$$\Phi = \left[\frac{A_s F_u n_u^2}{A_u F_s n_s^2}\right] \Phi_s$$

Φ = quantum yield (The quantum yield (Φ_s) for Coumarin 6 is 0.78 in EtOH)

s = coumarin 6

u = *o*-BzcDPE+H$^+$ or *p*-BzcDPE+H$^+$

A = absorbance

F = emission peak area

n = refractive index

Table. S7. Quantum yield data of *o*-BzcDPE+H$^+$ in different solvents.

Compound	Solvent	Absorbance (nm)	Emission peak (nm)	Φ (%)
o-BzcDPE+H$^+$	Toluene	285-410	478	20.9
	THF	240-410	478	9.8
	DCM	235-410	510	3.3
	ACN	215-415	516	0.46

Table. S8. Quantum yield data of *p*-BzcDPE+H$^+$ in different solvents.

Compound	Solvent	Absorbance (nm)	Emission peak (nm)	Φ (%)
p-BzcDPE+H$^+$	Toluene	240-430	466	60.9
	THF	230-455	507	34.6
	DCM	220-430	515	21.2
	ACN	200-455	563	0.65

Reference

[1] Secci D, Bolasco A, D'Ascenzio M, Della Sala F, Yáñez M, Carradori S. Conventional and Microwave-Assisted Synthesis of Benzimidazole Derivatives and TheirIn VitroInhibition of Human Cyclooxygenase. J Heterocycl Chem 2012;49:1187-95.

[2] Zhang G, Bai R-X, Li C-H, Feng C-G, Lin G-Q. Halogenation of 1,1-diarylethylenes by N-halosuccinimides. Tetrahedron 2019;75:1658-62.

[3] Matoliukstyte A, Burbulis E, Grazulevicius JV, Gaidelis V, Jankauskas V. Carbazole-containing enamines as charge transport materials for electrophotography. Synth Met 2008;158:462-7.

[4] Williams ATR, Winfield SA, Miller JN. Relative fluorescence quantum yields using a computer-controlled luminescence spectrometer. Analyst 1983;108:1067-71.